Redox-Dependent Structural Changes in an Engineered Heme−Copper Center in Myoglobin: Insights into Chloride Binding to Cu_B in Heme Copper Oxidases†

Xuan Zhao,‡ Mark J. Nilges,§ and Yi Lu*,‡

Department of Chemistry, University of Illinois at Urbana-Champaign, 600 South Mathews Avenue, Urbana, Illinois 61801, and The Illinois EPR Research Center, 506 South Mathews Avenue, Urbana, Illinois 61801

Received December 3, 2004; Revised Manuscript Received February 7, 2005

ABSTRACT: The effects of chloride on the redox properties of an engineered binuclear heme−copper center in myoglobin (Cu_BMb) were studied by UV−vis spectroelectrochemistry and EPR spectroscopy. A low-spin heme Fe^{III}−Cu^{I} intermediate was observed during the redox titration of Cu_BMb only in the presence of both Cu^{II} and chloride. Upon the first electron transfer to the Cu_B center, one of the His ligands of Cu_B center dissociates and coordinates to the heme iron, forming a six-coordinate low-spin ferric heme center and a reduced Cu_B center. The second electron transfer reduces the ferric heme and causes the release of the coordinated His ligand. Thus, the fully reduced state of the heme−copper center contains a five-coordinate ferrous heme and a reduced Cu_B center, ready for O_2 binding and reduction to water to occur. In the absence of a chloride ion, formation of the low-spin heme species was not observed. These redox reactions are completely reversible. These results indicate that binding of chloride to the Cu_B center can induce redox-dependent structural changes, and the bound chloride and hydroxide in the heme−copper center may play different roles in the redox-linked enzymatic reactions of heme−copper oxidases, probably because of their different binding affinity to the copper center and the relatively high concentration of chloride under physiological conditions.

Heme−copper oxidases (HCOs)[1] are a family of terminal oxidases that catalyze the reduction of O_2 to H_2O. During this reduction process, four protons are consumed to form two water molecules, while four additional protons are pumped across the membrane for the synthesis of ATP (*1*−*4*). The X-ray crystal structures of HCOs have been determined for several HCOs: the fully oxidized form from bovine heart (*5*−*9*), *Paracoccus denitrificans* (*10*, *11*), *T. sphaeroides* (*12*), *R. sphaeroides* (*13*), and quinol oxidase *bo*$_3$ (*14*), as well as the fully reduced form and the azide- and CO-bound forms from bovine heart (*15*). At the heart of the HCOs lies the binuclear heme−copper center where O_2 reduction occurs (Figure 1A). It consists of a high-spin heme a_3 with a proximal histidine ligand and, at ∼4.9 Å, a copper (Cu_B) coordinated to three histidines, one of which is cross-linked to tyrosine through a covalent bond.

Spectroscopic studies have shown that the heme−copper center contains a spin-coupled Cu^{II}−Fe^{III} site in its resting state, suggesting a possible bridging ligand between the heme and copper ion (*16*−*20*). This suggestion has been corroborated by observed electron density between the heme and copper center in X-ray structures of HCOs from bovine (*9*) and *Paracoccus denitrificans* (*11*). However, the exact identity of this bridging ligand remains to be defined. For example, a bridging peroxide has been proposed on the basis of the X-ray structure of HCO from bovine (*9*). The same electron density is also consistent with a hydroxide (or water) ligand to the Cu_B and a water or another weak-field ligand coordinated to the distal side of the heme (*11*). The latter proposal has been supported by spectroscopic studies (*21*−*25*).

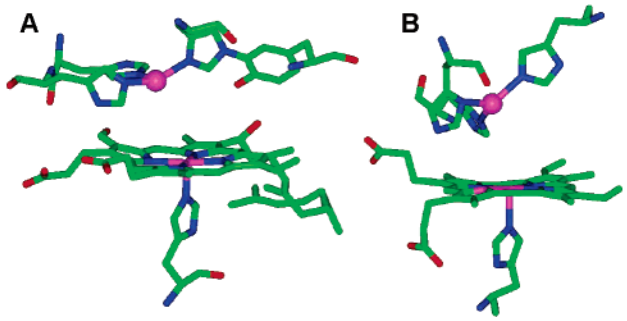

FIGURE 1: (A) Crystal structure of heme−copper center of bovine heart C*c*O (*9*). (B) Active site of a computer model of Cu_BMb.

A number of studies suggest chloride binding to the heme−copper center, probably as a ligand to Cu_B center, if the purification processes of HCOs are not rendered rigorously chloride-free (*26*). For example, early EXAFS studies suggested a heavy atom (S or Cl) bridging the heme a_3 and Cu_B (*27*−*29*). Assignment of the heavy atom to a chloride is preferred because sulfur-containing amino acid ligands can be excluded on the basis of X-ray structures (*5*−*14*) and no

† This material is based on work supported by the National Institutes of Health Grant GM62211.

* To whom correspondence should be addressed: Department of Chemistry, University of Illinois at Urbana-Champaign, Urbana, IL 61801. Telephone: (217) 333-2619. Fax: (217) 333-2685. E-mail: yi-lu@uiuc.edu.

‡ University of Illinois at Urbana-Champaign.

§ The Illinois EPR Research Center.

[1] Abbreviations: HCO, heme−copper oxidase; Mb, myoglobin; swMb, sperm whale myoglobin; Cu_BMb, F43H/L29HswMb; WT, wild type.

10.1021/bi047465c CCC: $30.25
Published on Web 04/05/2005

labile sulfur has been detected (*28*, *29*). The binding of chloride to the heme−copper center causes interesting changes in the spectroscopy and reactivity of the enzyme (*30*−*36*), such as lowering the redox potential of heme a_3 (*30*) and preventing fast reactions with CN^- (*34*) and NO (*35*). Furthermore, chloride has been found to bind to oxidized HCO in a 1:1 stoichiometry. The binding proceeds formally with the uptake of a proton and the bound chloride can be released into the medium after a single turnover (*26*, *37*). Finally, while most chloride-binding studies indicate only a weak-binding site, a recent EXAFS study suggests that chloride binds strongly to the fully reduced oxidase bound with CO (*23*). Reduction of the heme−copper center results in the loss of one of the three histidine ligands to Cu_B (*22*, *23*) and replacement of it by the tightly bound chloride that does not readily exchange with halide ions in the bulk solvent (*23*). The role of chloride in this redox-linked protonation of oxidase has also been studied by multiwavelength stopped-flow spectroscopy. The results indicate that chloride has no effect on the extent of proton uptake coupled to heme *a* reduction but significantly reduces the extent of uptake protons coupled to the reduction of the heme a_3−Cu_B center (*38*). On the basis of these studies, the possible role of chloride as a mimic of hydroxide ligand to the Cu_B center has been suggested (*23*, *38*).

While most of the above studies have focused on chloride binding to either fully oxidized (heme Fe^{III}−Cu^{II}) or fully reduced (heme Fe^{II}−Cu^{I}) forms, few reports have appeared on the characterization of chloride binding to the intermediate Fe^{III}−Cu^{I} form of the HCOs, probably because it is difficult to study such a transient species. Furthermore, the above studies indicate a need for further detailed characterization of intermediates during the reduction of the heme−copper center in the presence and absence of chloride and for defining the subtle differences between a chloride and hydroxide ligand to the Cu_B center. Toward this goal, we carried out spectroelectrochemical studies of an engineered heme−copper center constructed in sperm whale myoglobin (swMb) in the presence of chloride. This construction was accomplished by mutations of Phe43 and Leu29 to histidines in swMb. The two histidines, together with the distal His64 in the native swMb, form a binding site for Cu_B above the heme plane and in a similar position to heme−copper centers in native HCOs. The resulting engineered protein (F43H/L29HswMb, called Cu_BMb, Figure 1B) has been shown to bind 1 equiv of Cu^{2+} ion, which can be spin-coupled to the heme iron in the presence of ligands such as CN^- (*39*).

Myoglobin is one of the most well-characterized heme proteins. It has been proposed that several states in HCOs, such as oxy state **A**, have analogous counterparts in myoglobin (Mb), and reaction intermediates of HCOs are often compared with those in Mb (*40*). Designing and studying such a small model heme−copper protein in Mb that is free of other chromaphores complements well the studies of native HCOs by allowing easier characterization of complex intermediates of O_2 reduction and deducing more general principles about the heme protein structure and function. For example, previous studies of Cu_BMb have shown that the Cu_B center plays a critical role in O_2 binding and reduction and proton delivery plays an important role in the heterolytic O−O bond cleavage (*41*). Here, we report a new intermediate after the transfer of the first electron to the heme−copper center in Cu_BMb observed only in the presence of chloride. The implications of this finding on the role of chloride in redox-linked protonation and on its subtle differences with hydroxide will be discussed.

EXPERIMENTAL METHODS

Sample Preparations. The wild-type (WT) swMb and Cu_BMb proteins were expressed and purified as described previously (*39*). Phenazine methosulfate and anthraquinone-2-sulfonate were purchased from Sigma.

Spectroelectrochemical Measurements. The reduction potentials were measured by a spectroelectrochemical method using an optically transparent thin-layer cell (OTTLE) as described in details (*42*−*44*). The working electrode was made from a piece of 52 mesh platinum gauze. A 1 mm diameter platinum wire was used as the auxiliary electrode, while a piece of Pasteur pipet filled with agar gel containing 0.2 M K_2SO_4 was used as a salt bridge to connect the Ag/AgCl (3 M KCl) reference electrode to the bulk solution containing the working and auxiliary electrodes. Generally, the redox titration was performed using ~0.6 mL of working solution containing 0.2 mM protein, 40 μM phenazine methosulfate, and 40 μM anthraquinone-2-sulfonate as mediators. The working solution was purged gently with Ar for at least 30 min to remove O_2 before being transferred to the OTTLE cell.

A model 362 potentiostat from Princeton Applied Research was used to control the potential of the working electrode. After the potential was applied (typically with 25 mV increments), the UV−vis spectra were recorded using a Cary 3E spectrophotometer until no further spectral changes occurred. The Ag/AgCl (3 M KCl) reference electrode was calibrated with a SCE electrode and found to be 200 mV (versus NHE).

EPR Spectroscopy. EPR spectra were recorded on a Varian-122 X-band spectrometer equipped with an Air Products Helitran cryostat and temperature controller. Samples were prepared from bulk electrolysis of Cu_BMb solution under the same conditions as those for spectroelectrochemistry in the presence of 20% glycerol. After equilibrium was reached at an applied potential, about 400 μL of the electrolysis solution was transferred to an EPR tube via cannula under Ar and the samples were flash-frozen in liquid N_2 for EPR measurement.

Data Analysis. The spectroelectrochemical titration data over the entire spectra were analyzed by global analysis using singular value decomposition (SVD) and nonlinear regression modeling with SpecFit/32 (Spectrum Software Associates, Inc.). All of the data were fit with a model of A ↔ B because the Nernst plot at a single wavelength (e.g., 432 nm) is linear (see Figure 2) except for the redox titrations of Cu_BMb in the presence of both chloride and Cu^{II}, where the Nernst plot at a single wavelength (e.g., 432 nm) is nonlinear (see Figure 2B). Therefore, a model of A ↔ B ↔ C was used. The reduction potential of each protein was then obtained from the Nernst plot by plotting the applied potential versus the logarithm of the ratio of the oxidized to reduced forms of the protein from the global analysis of the entire spectra described above. Data analysis using a single wavelength (such as 432 nm) instead of the entire spectra resulted in

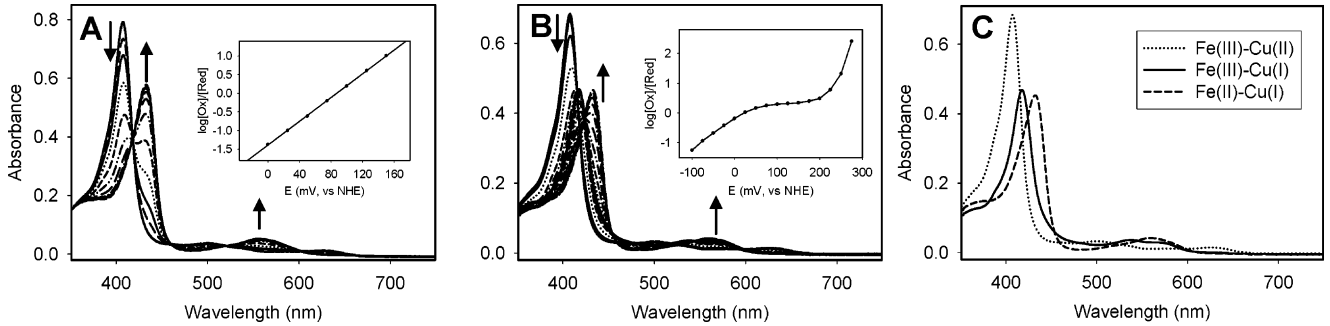

FIGURE 2: Spectroelectrochemical titration at 25 °C of (A) Cu_BMb in 20 mM Bis-Tris at pH 7 in the presence of 2 equiv of Cu^{II}, (B) Cu_BMb in 20 mM Bis-Tris at pH 7 in the presence of 5 equiv of Cu^{II} and 500 equiv of chloride. (Inset) Nernst plot from the dependence of the absorbance at 432 nm on the applied potential. The sweep potentials were applied in the negative direction. (C) UV−vis spectra of the fully oxidized heme $Fe^{III}-Cu^{II}$ (···), intermediate heme $Fe^{III}-Cu^{I}$ (—), and fully reduced heme $Fe^{II}-Cu^{I}$ (- - -) of chloride-bound Cu_BMb.

the same reduction potential within the error of the analysis (typically ±3 mV).

RESULTS AND DISCUSSION

The spectroelectrochemical reduction of oxidized Cu^{II}-bound Cu_BMb in 20 mM Bis-Tris at pH 7 resulted in decreases in absorptions at 408, 500, and 628 nm and increases in absorptions at 432 and 558 nm (Figure 2A). The clear isosbestic points at 418, 458, 524, and 600 nm indicate a clean conversion from the oxidized enzyme to the reduced enzyme, without any observable intermediates. The linear Nernst plot (inset of Figure 2A) is consistent with such a conclusion. A global analysis and fit of the entire spectra yielded a midpoint potential of 85 mV for the heme. A previous study showed that redox titrations of Cu^{II}-free Cu_B-Mb under the same condition resulted in the same reduction potential and similar spectral changes, i.e., decreases in absorptions at 408, 500, and 628 nm were accompanied by increases in absorptions at 432 and 558 nm, with clear isosbestic points at 418, 458, 524, and 600 nm. The result was attributed to the lack of spin coupling between the copper and the heme and thus little influence of reduction potential of the heme by the presence of the copper ion (*45*).

To explore the effects of chloride on the same process, the redox titration of Cu^{II}-free Cu_BMb was performed in the presence of 100 mM KCl and the heme redox potential of Cu_BMb was also found to be 82 mV (versus NHE), nearly the same as that in the absence of chloride, indicating that chloride does not bind to the heme in the absence of copper and thus has no direct effect on the heme redox potential. However, in the presence of both KCl and Cu^{II}, the redox titration of Cu_BMb yielded a nonlinear Nernst plot (Figure 2B), suggesting the presence of more than one redox process. The UV−vis spectra of the protein before reductive titration showed a Soret band at 408 nm and visible peaks at 500 and 628 nm, typical of a high-spin aqua-coordinated heme. Interestingly, an intermediate species appeared during the reductive titration, and it reached a maximum at 105 mV (versus NHE) (Figure 2B). The UV−vis spectra of this intermediate has absorptions at 418, 540, and 575 nm (Figure 2C), indicative of a low-spin ferric heme species. This species decreased under further negative potentials and was converted to the fully reduced species with a spectrum identical to that of the deoxy-Cu_BMb (Figure 2B). This redox process is completely reversible because reoxidation of the fully reduced protein resulted in the reverse spectral changes, through the same low-spin heme intermediate and back to the fully oxidized form.

The overall redox reaction can be fitted to two consecutive one-electron reduction processes using model A → B → C with $E_1 = 220$ mV (versus NHE) and $E_2 = -10$ mV (versus NHE). The first one-electron reduction process with a potential of $E_1 = 220$ mV (versus NHE) can be assigned to the reduction of Cu^{II} to Cu^{I}, because the Cu^{II}/Cu^{I} redox couple normally possesses a higher reduction potential than heme in Mb and because the UV−visible spectrum suggests that the heme was not reduced until the second one-electron reduction, as indicated in Figure 2B. Therefore, the species **B** can be assigned as heme $Fe^{III}-Cu^{I}$ and species **C** as heme $Fe^{II}-Cu^{I}$. In comparison to the heme potential in the absence of either Cu^{II} or chloride, the heme redox potential in the presence of both chloride and Cu^{II} was lowered from 85 to −10 mV, probably because of the formation of the low-spin species.

The formation of the heme $Fe^{III}-Cu^{I}$ species was also characterized by EPR spectroscopy. Before redox titration of a solution containing Cu_BMb (0.2 mM), KCl (100 mM), and Cu^{II} (1 mM), the EPR spectra showed the presence of both a high-spin heme Fe^{III} with rhombically split high-spin signals at $g = 6.08$ and 5.64 and Cu^{II} signals at $g = 2.22$ ($A = 160$ G), 2.05, and 2.01 (Figure 3A). In contrast to the cyanomet form of Cu_BMb (*39*), the presence of Cu^{II} had little effect on the ferric heme signals, suggesting that, without a bridging ligand such as cyanide, the presence of chloride in itself is not sufficient to result in spin coupling between Cu^{II} and ferric heme. This lack of spin coupling in the presence of halides is different from that of native HCOs; this difference could be due to a slightly different position of Cu^{II} relative to the heme iron, resulting in different orbital overlaps (*34*).

The bulk electrolysis of this solution with the applied potential at 105 mV (versus NHE) was conducted at 25 °C. After equilibrium was reached, a portion of the protein solution (~400 μL) was transferred to an EPR tube via cannula under Ar and frozen in liquid N_2. The EPR spectrum measured at 15 K is shown in Figure 3B. The strong Cu^{II} signals in Figure 3A decreased significantly, with a remaining minor signal at $g = 2.22$, 2.05, and 2.01 amounting to less than 5% of the original copper concentration. The disappearance of the Cu^{II} signal is consistent with the assignment of heme $Fe^{III}-Cu^{I}$ for this intermediate based on the UV−vis titration data. In addition, the high-spin heme signal at *g*

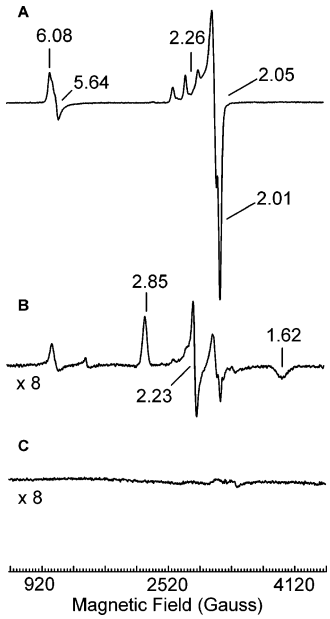

FIGURE 3: X-band EPR spectra of (A) fully oxidized heme $Fe^{III}-Cu^{II}$, (B) intermediate heme $Fe^{III}-Cu^{I}$, and (C) fully reduced heme $Fe^{II}-Cu^{I}$ of chloride-bound Cu_BMb. The samples were in 20 mM Bis-Tris at pH 7. The spectra were recorded at 15 K with a microwave power of 0.2 mW and a microwave frequency of 9.050 GHz.

$= 5.63$ decreased dramatically and new signals at $g = 2.85$, 2.23, and 1.62 appeared, suggesting formation of a low-spin ferric species, again in agreement with the UV−vis spectral analysis. Another minor species with $g = 4.23$ could be due to heme decomposition. These EPR signals are typical of the low-spin H-type hemoglobin coordinated by a distal histidine with a deprotonated N-1 (N_3 imidazole, N_1^-; $g =$ 2.80, 2.26, and 1.67) and bis-His-coordinated cytochrome b_5 at high pH conditions (*46*−*49*). When the bulk electrolysis was conducted at further negative potential [−200 mV (versus NHE)], the low-spin signal disappeared because of the formation of the fully reduced EPR-silent heme $Fe^{II}-Cu^{I}$ center (Figure 3C). The UV−vis spectrum of this fully reduced state resembles that of a five-coordinate reduced heme, indicating that one of the histidine ligands to the heme in the heme $Fe^{III}-Cu^{I}$ state dissociated from the heme center upon the full reduction of heme.

As discussed in the introduction, a number of studies have indicated chloride binding to the heme copper center, and the binding plays a role in redox-linked protonation. Although the exact chloride-binding mode remains to be defined structurally, chloride has been proposed to serve as a ligand of the Cu_B center (Scheme 1), analogous to the hydroxide ligand found by EXAFS and ENDOR studies (*21*−*23*, *38*). It was further proposed that reduction of the Cu_B center resulted in protonation of chloride and release of HCl in the solution, again in an analogous way as protonation of hydroxide and release of H_2O (Scheme 1) (*38*). When a heme−copper center in a small, well-characterized myoglobin was engineered, this study revealed three new findings. First, a new low-spin coordinated intermediate was identified and characterized by UV−vis and EPR on the heme $Fe^{III}-Cu^{I}$ form in the presence of chloride. Recent EXAFS studies of cytochrome bo_3 oxidases have shown that one of the histidine ligands to the Cu_B center became dissociated from the copper upon reduction (*23*, *38*). The observation of a low-spin heme in Cu_BMb upon reduction indicates that this dissociated histidine may coordinate to the heme in the heme $Fe^{III}-Cu^{I}$ form when chloride is present. However, the dissociated histidine does not coordinate to the heme when the protein is fully reduced to heme $Fe^{II}-Cu^{I}$, because the fully reduced form optically resembles that of deoxymyoglobin (Scheme 1).

An earlier study showed the binding of chloride lowered the reduction potential of the heme in the heme−copper center of native HCOs (*30*). The spectroelectrochemical titrations of Cu_BMb showed that the heme potential remained the same in the absence of copper ion in the Cu_B center and can be lowered by 95 mV only in the presence of *both* chloride and copper. Although both the negative charge on the chloride ion and the positive charge on the copper ion can influence the heme reduction potential, especially when the copper is spin-coupled to the heme center, their effects are generally small (*45*). Previous studies on other heme proteins with axial heme ligation have shown that the heme potential can be lowered by 171 (*50*) and 182 mV (*51*) through coordination of another histidine to heme. Therefore, we believe that the main factor for lowering the reduction potential is a spin transition from high to low spin.

Scheme 1: Redox-Dependent Structural Changes of the Cu_B Center (A) in the Absence of Chloride and (B) in the Presence of Excess Chloide

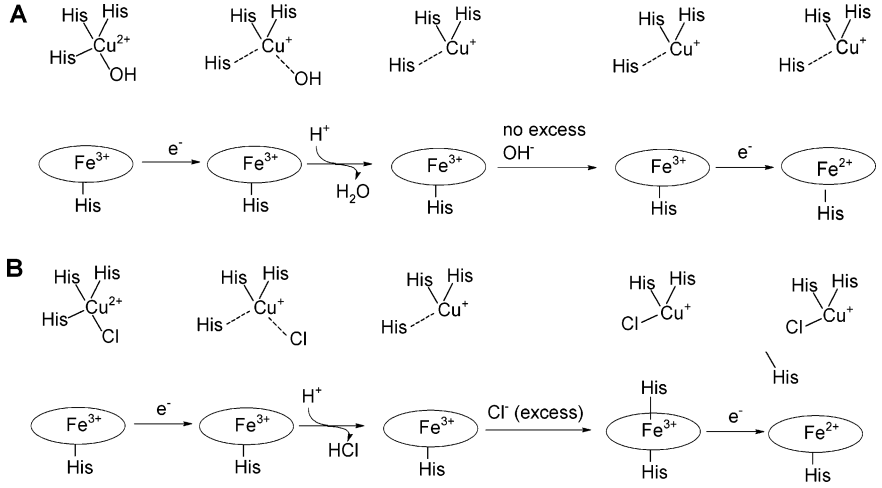

Finally, the low-spin bis-His-coordinated heme was not observed in the absence of chloride, suggesting different roles played between hydroxide and chloride as a ligand to the Cu_B center. This difference in the intermediate may explain their different reactivities. For example, previous studies of cytochrome oxidases showed that chloride binding prevents fast reactions with CN^- and NO (*34*, *35*). Because chloride does not bind to the heme in the heme copper center, it is not clear how it can have such a dramatic influence on CN^- and NO binding to the heme. EXAFS studies of cytochrome bo_3 from *Escherichia coli* indicated that reduction of the binuclear center weakens both the coordinated water molecule and one of the Cu_B-histidine ligands (*22*, *23*). A major difference between chloride and hydroxide is their effective concentrations at physiological pH; chloride concentration is normally as high as 25 mM, while hydroxide is much lower (~0.3 μM at pH 7.5). Water is a weaker ligand for Cu^I than either histidine or chloride, and thus is unlikely to substitute for a bound histidine unless converted to hydroxide. Despite the low physiological concentration of hydroxide, the existence of a copper-bound hydroxide is still possible because of the expected lowering of the pK_a of a copper-bound water molecule to the range 6−8. However, the change in pK_a is much less pronounced for the less positive Cu^I, so formation of a copper hydroxide is unlikely. Therefore, the combined effects of the high physiological concentration of chloride and the only slightly reduced pK_a of water bound to Cu^I makes it likely that the coordination of chloride is solely responsible for the dissociation of the loosely bound histidine ligand, which in turn binds to the heme making the six-coordinate intermediate. Control experiments in our system in which the six-coordinate species was not observed in the absence of chloride confirm this conclusion as any copper hydroxide species generated from a lowering of the pK_a of water should form regardless of the concentration of chloride ion.

Our findings and explanations in Scheme 1 are consistent with previous EXAFS results (*22*, *23*). In the chloride-free form of the fully reduced cytochrome bo_3 oxidase, the weakly bound His ligand to Cu_B was found to be only slightly further away from the Cu_B center (at 2.10 Å) than the two strongly bound His ligands (at 1.92 Å), not enough perturbation for the His to coordinate to the heme. On the other hand, in the chloride-bound form of the CO derivative of the reduced cytochrome bo_3 oxidase, the His residue was found to be so far away from the Cu_B center that it was no longer detectable by EXAFS (*22*, *23*). Our findings here suggest that this His residue could coordinate to the heme to form the low-spin species observed in HCOs. Furthermore, we propose a different binding affinity to the copper center, and the relatively high concentration of chloride under physiological conditions may contribute the different roles that chloride and hydroxide play in the HCO; high concentration of chloride can replace the His, whose binding to the heme resulted in formation of the low-spin heme species that makes the heme coordination saturated and not capable of binding to other ligands.

CONCLUSIONS

The redox titration of the $Fe^{III}-Cu^{II}$ center in Cu_BMb in the presence of both chloride and Cu^{II} showed that one of the His ligands dissociated from the Cu_B center upon the first electron reduction and coordinated to the heme center to form a low-spin heme $Fe^{III}-Cu^I$ intermediate. This low-spin species was not observed in the absence of either chloride or Cu^{II}. Further reduction of the heme $Fe^{III}-Cu^I$ form resulted in the release of the coordinated His from the heme center and five-coordinate high-spin heme $Fe^{II}-Cu^I$ species. These results demonstrate that chloride can bind to the Cu_B center and play an important role in the redox processes of the heme−copper center and that the bound chloride and hydroxide in the heme−copper center may play slightly different roles in the reduction of the heme−copper center of HCOs. Factors may include a different binding affinity to the copper center and the relatively high concentration of chloride under physiological conditions. These factors should be considered when discussing their roles in HCOs.

ACKNOWLEDGMENT

We thank Professor Takashi Hayashi and Dr. Joel E. Morgan for advice on spectroelectrochemical cells and Professor Andrew A. Gewirth for helpful discussions.

REFERENCES

1. Babcock, G. T., and Wikström, M. (1992) Oxygen activation and the conservation of energy in cell respiration, *Nature 356*, 301−309.
2. Garcia-Horsman, J. A., Barquera, B., Rumbley, J., Ma, J., and Gennis, R. B. (1994) The superfamily of heme−copper respiratory oxidases, *J. Bacteriol. 176*, 5587−5600.
3. Ferguson-Miller, S., and Babcock, G. T. (1996) Heme/copper terminal oxidases, *Chem. Rev. 96*, 2889−2907.
4. Namslauer, A., and Brzezinski, P. (2004) Structural elements involved in electron-coupled proton transfer in cytochrome *c* oxidase, *FEBS Lett. 567*, 103−110.
5. Yoshikawa, S., Shinzawa-Itoh, K., and Tsukihara, T. (2000) X-ray structure and the reaction mechanism of bovine heart cytochrome *c* oxidase, *J. Inorg. Biochem. 82*, 1−7.
6. Yoshikawa, S., Shinzawa-Itoh, K., and Tsukihara, T. (1998) Crystal structure of bovine heart cytochrome *c* oxidase at 2.8 Å resolution, *J. Bioenerg. Biomembr. 30*, 7−14.
7. Tsukihara, T., Aoyama, H., Yamashita, E., Tomizaki, T., Yamaguchi, H., Shinzawa-Itoh, K., Nakashima, R., Yaono, R., and Yoshikawa, S. (1995) Structures of metal sites of oxidized bovine heart cytochrome *c* oxidase at 2.8 Å, *Science 269*, 1069−1074.
8. Tsukihara, T., Aoyama, H., Yamashita, E., Tomizaki, T., Yamaguchi, H., Shinzawa-Itoh, K., Nakashima, R., Yaono, R., and Yoshikawa, S. (1996) The whole structure of the 13-subunit oxidized cytochrome *c* oxidase at 2.8 Å, *Science 272*, 1136−1144.
9. Yoshikawa, S., Shinzawa-Itoh, K., Nakashima, R., Yaono, R., Yamashita, E., Inoue, N., Yao, M., Fei, M. J., Libeu, C. P., Mizushima, T., Yamaguchi, H., Tomizaki, T., and Tsukihara, T. (1998) Redox-coupled crystal structural changes in bovine heart cytochrome *c* oxidase, *Science 280*, 1723−1729.
10. Iwata, S., Ostermeier, C., Ludwig, B., and Michel, H. (1995) Structure at 2.8 Å resolution of cytochrome *c* oxidase from *Paracoccus denitrificans*, *Nature 376*, 660−669.
11. Ostermeier, C., Harrenga, A., Ermler, U., and Michel, H. (1997) Structure at 2.7 Å resolution of the *Paracoccus denitrificans* two-subunit cytochrome *c* oxidase complexed with an antibody Fv fragment, *Proc. Natl. Acad. Sci. U.S.A. 94*, 10547−10553.
12. Soulimane, T., Buse, G., Bourenkov, G. P., Bartunik, H. D., Huber, R., and Than, M. E. (2000) Structure and mechanism of the aberrant ba_3-cytochrome *c* oxidase from *Thermus thermophilus*, *EMBO J. 19*, 1766−1776.
13. Svensson-Ek, M., Abramson, J., Larsson, G., Tornroth, S., Brzezinski, P., and Iwata, S. (2002) The X-ray crystal structures of wild-type and EQ(I-286) mutant cytochrome *c* oxidases from *Rhodobacter sphaeroides*, *J. Mol. Biol. 321*, 329−339.
14. Abramson, J., Riistama, S., Larsson, G., Jasaitis, A., Svensson-Ek, M., Laakkonen, L., Puustinen, A., Iwata, S., and Wikstrom,

M. (2000) The structure of the ubiquinol oxidase from *Escherichia coli* and its ubiquinone binding site, *Nat. Struct. Biol. 7*, 910−917.
15. Fei, M. J., Yamashita, E., Inoue, N., Yao, M., Yamaguchi, H., Tsukihara, T., Shinzawa-Itoh, K., Nakashima, R., and Yoshikawa, S. (2000) X-ray structure of azide-bound fully oxidized cytochrome *c* oxidase from bovine heart at 2.9 Å resolution, *Acta Crystallogr., Sect. D 56*, 529−535.
16. Shaw, R. W., Hansen, R. E., and Beinert, H. (1978) A novel electron paramagnetic resonance signal of "oxygenated" cytochrome *c* oxidase, *J. Biol. Chem. 253*, 6637−6640.
17. Brudvig, G. W., Stevens, T. H., Morse, R. H., and Chan, S. I. (1981) Conformations of oxidized cytochrome *c* oxidase, *Biochemistry 20*, 3912−3921.
18. Salerno, J. C., Bolgiano, B., Poole, R. K., Gennis, R. B., and Ingledew, W. J. (1990) Heme−copper and heme−heme interactions in the cytochrome *bo*-containing quinol oxidase of *Escherichia coli*, *J. Biol. Chem. 265*, 4364−4368.
19. Watmough, N. J., Cheesman, M. R., Gennis, R. B., Greenwood, C., and Thomson, A. J. (1993) Distinct forms of the heme *o*-Cu binuclear site of oxidized cytochrome *bo* from *Escherichia coli*. Evidence from optical and EPR spectroscopy, *FEBS Lett. 319*, 151−154.
20. Day, E. P., Peterson, J., Sendova, M. S., Schoonover, J., and Palmer, G. (1993) Magnetization of fast and slow oxidized cytochrome *c* oxidase, *Biochemistry 32*, 7855−7860.
21. Fann, Y. C., Ahmed, I., Blackburn, N. J., Boswell, J. S., Verkhovskaya, M. L., Hoffman, B. M., and Wikström, M. (1995) Structure of Cu_B in the binuclear heme−copper center of the cytochrome aa_3-type quinol oxidase from *Bacillus subtilis*: An ENDOR and EXAFS study, *Biochemistry 34*, 10245−10255.
22. Osborne, J. P., Cosper, N. J., Staelhandske, C. M. V., Scott, R. A., Alben, J. O., and Gennis, R. B. (1999) Cu XAS shows a change in the ligation of Cu_B upon reduction of cytochrome bo_3 from *Escherichia coli*, *Biochemistry 38*, 4526−4532.
23. Ralle, M., Verkhovskaya, M. L., Morgan, J. E., Verkhovsky, M. I., Wikstroem, M., and Blackburn, N. J. (1999) Coordination of Cu_B in reduced and CO-liganded states of cytochrome bo_3 from *Escherichia coli*. Is chloride ion a cofactor? *Biochemistry 38*, 7185−7194.
24. Han, S., Ching, Y. C., and Rousseau, D. L. (1990) Ferryl and hydroxy intermediates in the reaction of oxygen with reduced cytochrome *c* oxidase, *Nature 348*, 89−90.
25. Han, S., Takahashi, S., and Rousseau, D. L. (2000) Time dependence of the catalytic intermediates in cytochrome *c* oxidase, *J. Biol. Chem. 275*, 1910−1919.
26. Fabian, M., Skultety, L., Jancura, D., and Palmer, G. (2004) Implications of ligand binding studies for the catalytic mechanism of cytochrome *c* oxidase, *Biochim. Biophys. Acta 1655*, 298−305.
27. Li, P. M., Gelles, J., Chan, S. I., Sullivan, R. J., and Scott, R. A. (1987) Extended X-ray absorption fine structure of copper in CuA-depleted, *p*-(hydroxymercuri)benzoate-modified, and native cytochrome *c* oxidase, *Biochemistry 26*, 2091−2095.
28. Scott, R. A., Li, P. M., and Chan, S. I. (1988) The binuclear site of cytochrome *c* oxidase. Structural evidence from iron X-ray absorption spectroscopy, *Ann. N. Y. Acad. Sci. 550*, 53−58.
29. Powers, L., Lauraeus, M., Reddy, K. S., Chance, B., and Wikstroem, M. (1994) Structure of the binuclear heme iron−copper site in the quinol-oxidizing cytochrome aa_3 from *Bacillus subtilis*, *Biochim. Biophys. Acta 1183*, 504−512.
30. Blair, D. F., Ellis, W. R., Jr., Wang, H., Gray, H. B., and Chan, S. I. (1986) Spectroelectrochemical study of cytochrome *c* oxidase: pH and temperature dependences of the cytochrome potentials. Chacterization of site−site interactions, *J. Biol. Chem. 261*, 11524−11537.
31. Moody, A. J., Cooper, C. E., and Rich, P. R. (1991) Characterization of "fast" and "slow" forms of bovine heart cytochrome-*c* oxidase, *Biochim. Biophys. Acta 1059*, 189−207.
32. Geier, B. M., Schaegger, H., Ortwein, C., Link, T. A., Hagen, W. R., Brandt, U., and von Jagow, G. (1995) Kinetic properties and ligand binding of the eleven-subunit cytochrome-*c* oxidase from *Saccharomyces cerevisiae* isolated with a novel large-scale purification method, *Eur. J. Biochem. 227*, 296−302.
33. Hirano, T., Mogi, T., Tsubaki, M., Hori, H., Orii, Y., and Anraku, Y. (1997) A novel chloride-binding site modulates the heme−copper binuclear center of the *Escherichia coli bo*-type ubiquinol oxidase, *J. Biochem. 122*, 430−437.
34. Moody, A. J., Butler, C. S., Watmough, N. J., Thomson, A. J., and Rich, P. R. (1998) The reaction of halides with pulsed cytochrome *bo* from *Escherichia coli*, *Biochem. J. 331*, 459−464.
35. Giuffre, A., Stubauer, G., Brunori, M., Sarti, P., Torres, J., and Wilson, M. T. (1998) Chloride bound to oxidized cytochrome *c* oxidase controls the reaction with nitric oxide, *J. Biol. Chem. 273*, 32475−32478.
36. Cheesman, M. R., Oganesyan, V. S., Watmough, N. J., Butler, C. S., and Thomson, A. J. (2004) The nature of the exchange coupling between high-spin Fe^{III} heme o_3 and Cu_B^{II} in *Escherichia coli* quinol oxidase, cytochrome bo_3: MCD and EPR studies, *J. Am. Chem. Soc. 126*, 4157−4166.
37. Fabian, M., Skultety, L., Brunel, C., and Palmer, G. (2001) Cyanide stimulated dissociation of chloride from the catalytic center of oxidized cytochrome *c* oxidase, *Biochemistry 40*, 6061−6069.
38. Forte, E., Barone, M. C., Brunori, M., Sarti, P., and Giuffre, A. (2002) Redox-linked protonation of cytochrome *c* oxidase: The effect of chloride bound to CuB, *Biochemistry 41*, 13046−13052.
39. Sigman, J. A., Kwok, B. C., and Lu, Y. (2000) From myoglobin to heme−copper oxidase: Design and engineering of a Cu_B center into sperm whale myoglobin, *J. Am. Chem. Soc. 122*, 8192−8196.
40. Veselov, A. V., Osborne, J. P., Gennis, R. B., and Scholes, C. P. (2000) Q-Band ENDOR (electron nuclear double resonance) of the heme o3 liganding environment at the binuclear center in cytochrome bo_3 from *Escherichia coli*, *J. Am. Chem. Soc. 122*, 8712−8716.
41. Sigman, J. A., Kim, H. K., Zhao, X., Carey, J. R., and Lu, Y. (2003) The role of copper and protons in heme−copper oxidases: Kinetic study of an engineered heme−copper center in myoglobin, *Proc. Natl. Acad. Sci. U.S.A. 100*, 3629−3634.
42. Taboy, C. H., Bonaventura, C., and Crumbliss, A. L. (2002) Anaerobic oxidations of myoglobin and hemoglobin by spectroelectrochemistry, *Methods Enzymol. 353*, 187−209.
43. Matsuo, T., Dejima, H., Hirota, S., Murata, D., Sato, H., Ikegami, T., Hori, H., Hisaeda, Y., and Hayashi, T. (2004) Ligand binding properties of myoglobin reconstituted with iron porphycene: Unusual O_2 binding selectivity against CO binding, *J. Am. Chem. Soc. 126*, 16007−16017.
44. Hayashi, T., Dejima, H., Matsuo, T., Sato, H., Murata, D., and Hisaeda, Y. (2002) Blue myoglobin reconstituted with an iron porphycene shows extremely high oxygen affinity, *J. Am. Chem. Soc. 124*, 11226−11227.
45. Zhao, X., Yeung, N., Wang, Z., Guo, Z., and Lu, Y. (2005) Effects of metal ions in the CuB center on the redox properties of heme in heme−copper oxidases: Spectroelectrochemical studies of an engineered heme−copper center in myoglobin, *Biochemistry 44*, 1210−1214.
46. Peisach, J., Blumberg, W. E., Wittenberg, B. A., Wittenberg, J. B., and Kampa, L. (1969) Hemoglobin A: Electron paramagnetic resonance study of the effects of interchain contacts on the heme symmetry of high-spin and low-spin derivatives of ferric α chains, *Proc. Natl. Acad. Sci. U.S.A. 63*, 934−939.
47. Bois-Poltoratsky, R., and Ehrenberg, A. (1967) Magnetic and spectrophotometric investigations of cytochrome b_5, *Eur. J. Biochem. 2*, 361−365.
48. Ikeda, M., Iizuka, T., Takao, H., and Hagihara, B. (1974) Studies on the heme environment of oxidized cytochrome b_5, *Biochim. Biophys. Acta 336*, 15−24.
49. Svistunenko, D. A., Sharpe, M. A., Nicholls, P., Blenkinsop, C., Davies, N. A., Dunne, J., Wilson, M. T., and Cooper, C. E. (2000) The pH dependence of naturally occurring low-spin forms of methaemoglobin and metmyoglobin: An EPR study, *Biochem. J. 351*, 595−605.
50. Lloyd, E., Hildebrand, D. P., Tu, K. M., and Mauk, A. G. (1995) Conversion of myoglobin into a reversible electron-transfer protein that maintains bishistidine axial ligation, *J. Am. Chem. Soc. 117*, 6434−6438.
51. Dou, Y., Admiraal, S. J., Ikeda-Saito, M., Krzywda, S., Wilkinson, A. J., Li, T., Olson, J. S., Prince, R. C., Pickering, I. J., et al. (1995) Alteration of axial coordination by protein engineering in myoglobin. Bisimidazole ligation in the His64 → Val/Val68 → His double mutant, *J. Biol. Chem. 270*, 15993−16001.

BI047465C